INTERNATIONAL JOURNAL OF HYDROGEN ENERGY 41 (2016) 21503–21515

Available online at www.sciencedirect.com

ScienceDirect

journal homepage: www.elsevier.com/locate/he

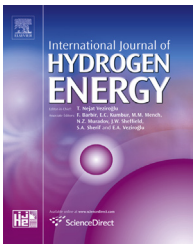

An Energy Management Strategy to concurrently optimise fuel consumption & PEM fuel cell lifetime in a hybrid vehicle

Tom Fletcher [a,*], *Rob Thring* [a], *Martin Watkinson* [b]

[a] AACME, Loughborough University, Loughborough, LE11 3TU, UK
[b] HORIBA-MIRA, Watling Street, Nuneaton, Warwickshire, CV10 0TU, UK

ARTICLE INFO

Article history:
Received 11 June 2016
Received in revised form
18 August 2016
Accepted 22 August 2016
Available online 8 September 2016

Keywords:
Energy Management Strategy
Stochastic Dynamic Programming
Hybrid vehicle
Fuel cell
Reliability
Cost

ABSTRACT

The cost and reliability of fuel cells are major obstructions preventing fuel cell hybrid electric vehicle (FCHEV) from entering the mainstream market. However, many of the degradation methods are strongly affected by the operating conditions of the fuel cell and therefore can be mitigated by optimisation of the Energy Management Strategy (EMS). The major causes of fuel cell degradation are identified from the literature and a model is produced in order to estimate the effect of the EMS on the fuel cell degradation. This is used to produce an optimal strategy for a low speed campus vehicle using Stochastic Dynamic Programming (SDP). The SDP controller attempts to minimise the total running cost of the fuel cell, inclusive of both fuel consumption and degradation, each weighted by their respective costs. The new strategy is shown to increase the lifetime of the fuel cell by 14%, with only a 3.5% increase in fuel consumption, largely by avoiding transient loading on the fuel cell stack.

Introduction

The optimisation of an Energy Management Strategy (EMS) seeks to maximise the benefits afforded by inclusion of an energy storage medium on board a Hybrid Electric Vehicle (HEV). Some of these benefits are immediately obvious, such as the ability to re-capture kinetic energy which would otherwise be lost as heat during braking. However, further gains can be made by optimising the operating points of various components in the vehicle in order to maximise the efficiency of the system in a holistic sense [1–3]. As with any optimisation problem, there is often a degree of "trade-off" between various targets which may include fuel consumption, emissions, drive-ability and component degradation. The techniques used for the optimisation of the EMS for a Fuel Cell Hybrid Electric Vehicle (FCHEV) is very similar to that of an Internal Combustion Engine (ICE) powered HEV, however the targets of the cost function do vary. For example, emissions are not an issue for Proton Exchange Membrane (PEM) fuel cells running on pure hydrogen, and drive-ability concerns [4–6], such as the timing of gear changes, are not applicable to the majority of pure electric drive-train designs.

Current energy management techniques for hybrid vehicles focus heavily on the fuel consumption. For an ICE HEV, this makes sense as the efficiency varies considerably over power range, however the efficiency curve of a fuel cell stack

* *Corresponding author.*
E-mail addresses: T.P.Fletcher@lboro.ac.uk (T. Fletcher), R.H.Thring@lboro.ac.uk (R. Thring), martin.watkinson@horiba-mira.com (M. Watkinson).

http://dx.doi.org/10.1016/j.ijhydene.2016.08.157

tends to be much flatter [7], meaning that its operating efficiency is much less dependent on the actions of the EMS. More importantly, the high cost of the fuel cell, and its relatively low durability, are of concern in a FCHEV and therefore should be included in the optimisation process.

Motivation

The high cost of fuel cells is one of the major obstructions preventing FCHEV from entering the mainstream transport market. Fuel cells are estimated as costing well over $50/kW (under mass production) [8] compared to a US Department of Energy (DoE) target of approximately $35/kW [9] in order to become competitive with ICEs. This issue is compounded by the relatively poor reliability of fuel cell stacks when compared to conventional technology. The fuel cell used in our test vehicle is rated to 1500 h, well below the 5000 h of service target from the DoE for transport applications [9]. Combined with their high cost, this means the overall lifetime cost of running a FCHEV is not yet competitive with conventional powertrain designs.

These issues are strongly inter-related. The cost of the fuel cell can be reduced, for example, by reducing the platinum loading on the catalyst layer, however this will tend to affect the long-term performance of the cell and therefore reduce its usable lifetime. The cost of the system could also be reduced by using a smaller stack and running it at a higher relative power, however this will also tend to reduce the efficiency and increase the rates of degradation and therefore reduce the lifetime of the system. This means that it is hard to gauge whether the initial cost saving of using a lower platinum loading or a smaller stack will be outweighed by the increased maintenance cost due to the reduced reliability.

It is therefore imperative to manage the fuel cell stack in such a way as to maximise its reliability in order to minimise the lifetime cost of the vehicle. The reliability of a fuel cell stack depends to a large degree on how it is used [10,11]. Certain actions, such as frequent start-stop cycling and high current loading can significantly reduce the lifetime of the stack [11,12]. Due to the high cost of the fuel cell stack and its sensitivity to the operating conditions determined by the EMS, it makes sense to include the anticipated degradation in a quantitative sense.

Proposed solution

This can be achieved using current optimisation techniques, such as dynamic programming, by modifying the cost function to include not only the fuel consumption, but also the expected fuel cell degradation that will occur as a result of the EMS actions. The two performance metrics can be weighted by their associated costs in order to minimise the overall running cost of the vehicle.

In addition to optimising the true running cost of the vehicle, rather than just fuel economy, the associated increase in reliability should also bring fuel cell vehicles closer to the US Department of Energy's target of 5000 h of operation [9] in order to be competitive with conventional technology. An effective EMS has the potential to not only increase the useful lifetime of the fuel cell by avoiding actions known to cause degradation, but also due to a reduction in the average power requirements as a result of the optimisation of system efficiency.

Prior literature

Two main development paths have been explored when researching this problem. The first is how to optimise the Energy Management Strategy (EMS). A very good overview of optimal energy management strategies can be found in the April 2007 IEEE Control Systems Magazine by Sciarretta and Guzzella [13]. This work concentrates on ICE HEVs, but much of the work is appropriate to FCHEVs as well. According to Sciarretta and Guzzella, achievable improvements in fuel consumption can be as high as 30% over conventional vehicles, but improvements of this magnitude can only be realised with sophisticated control systems.

The simplest strategies are those used in practical situations, especially industrial applications [14,15], where the emphasis is to get a vehicle up and running as quickly as possible. Generally under these circumstances, the EMS strategy is based on a number of hard coded heuristic rules, for example increasing the engine/fuel cell power when the battery State of Charge (SoC) is low. Heuristic controllers vary greatly in complexity [15,16] and performance, but are generally very robust and quick to implement in real-time [17]. Unfortunately, they often require manual tuning and therefore can be very time consuming to optimise.

In addition to heuristic controllers, there are a number of works utilising machine learning techniques in order to optimise the EMS such as neural networks [18], game theory [19], and dynamic programming [1,20–22]. These techniques generally use a model of the vehicle in order to optimise the control strategy using a cost function. As a result, they generally produce better results than heuristic controllers. Two main techniques, however, have come to the forefront in recent years, Equivalent Consumption Minimization Strategy (ECMS) [5,23–32] and Stochastic Dynamic Programming (SDP) [6,14,32–40].

The first proposal of SDP is usually credited to Lin et al. [34] as means to produce an optimised, causal and time-invariant EMS which could therefore be implemented on board the vehicle for real-time control. Since 2004, SDP has been used by a number of authors for ICE HEVs [38,39,41,42] and more recently FCHEVs [14,35] and has been gradually refined by the use of more complex models, improved cost functions to include emissions, drive-ability and battery degradation [38,40] and more advanced solving algorithms such as "terminal state" SDP [42].

The vast majority of research into the EMS focuses solely on improving the fuel economy of the vehicle [1,7,14–16,21,28,29,33–36,39,41–45], although for ICE hybrid vehicles, authors have also included factors such as emissions [19], and drive-ability [5,6,37]. Research into EMS strategy for FCHEV specific issues generally lags behind in this regard.

A number of authors have proposed EMSs that combat fuel cell degradation, mainly focussed on two major causes; the reduction of transient loading, and prevention of reactant starvation. Thounthong et al. [46,47] and more recently Aouzellag et al. [48] target the reduction of transient loading with a "rule-based" approach using rate of load change limits on the

fuel cell and the battery pack. Pukrushpan et al. [49], Vahidi et al. [50] and Lin et al. [35] focus on the control of oxygen flow in order to prevent reactant starvation. More recently, Xu et al. [51] has developed a multi-mode strategy that includes limitations on the upper and lower fuel cell power as well as the reduction of transient loads by using penalty functions on a Deterministic Dynamic Programming (DDP) optimisation.

The second area of research relevant to this work is the degradation of fuel cells. There is a large volume of research concerning the degradation of fuel cells ranging from detailed electrochemical modelling [52] to empirical work on accelerated ageing testing [11,53]. A number of reasons for fuel cell degradation have been identified including degradation of catalyst layer ("Electro-Chemical Active Surface Area (ECASA)" reduction) [11,53], membrane chemical attack [11,53], hydrothermal mechanic stress on the membrane [54] and thermal degradation of the membrane [11,50,55,56]. A comprehensive review of fuel cell degradation methods has been included in the next section.

Contributions

The main objective of this paper is to develop previous work [57] using SDP on FCHEVs to optimally "trade-off" fuel consumption and cell degradation. This work is believed to be the first to quantitatively consider the effect of the EMS on the voltage degradation of the fuel cell and optimise the actions of the fuel cell based on overall running cost.

Firstly the inclusion of multiple degradation methods will allow a better estimation of the true fuel cell lifetime, especially under circumstances where degradation methods may "compete" with each other. Secondly, the estimation of the fuel cell lifetime will allow a new method for choosing weighting parameters between degradation and fuel costs using effective fuel cell running cost projection.

A review of fuel cell degradation methods

The EMS is not directly responsible for managing the fuel cell; however the decisions it makes can significantly affect the conditions in the stack [51,54,58,59]. For example, running the fuel cell at high current densities for long periods of time may exceed the cooling capabilities of the stack ancillaries. Highly transient loading can also negatively affect the homoeostasis of temperature and humidity in the membrane [53] resulting in localised degradation. This section will begin with a review of the most well-known causes of Membrane Electrode Assembly (MEA) performance degradation, which can be split into three categories; catalyst layer, membrane, and Gas Diffusion Layer (GDL).

Fuel cell degradation methods

Catalyst degradation

The EMS has a significant impact on fuel cell degradation due to ECASA reduction. Under ideal conditions, high numbers of platinum catalyst particles will be spread evenly over the support material maximising their active surface area. However, over time, these particles will tend to agglomerate, sinter together or detach entirely from the support, gradually reducing the surface area and hence cell voltage [60]. This process can be accelerated under certain conditions, such as fuel starvation, which may lead to oxidation of the carbon support [12]. Fuel starvation may be caused by exceeding the maximum reactant supply rates when running under high current loading, but localised fuel starvation can also result due to transient loading or during start-up and shut-down procedures [11,53,61]. Another major cause of catalyst layer degradation occurs when running at very low current densities. High cathode potentials can cause an increase in the surface oxides on the platinum particles leading to a loss of activity and potential agglomeration when they are reduced [62], see Fig. 1.

Membrane degradation

The degradation of the membrane is generally originates from chemical attack, mechanical stress and/or thermal stress [11,12,53]. Chemical attack is generally caused by contaminants in the fuel [12]. Mechanical stress is generally caused by improper assembly or by congenital defects [11,12]. The EMS can do very little to prevent these causes, but thermal stress can be mitigated by running the fuel cell at its ideal operating point. High levels of heat may cause a drop in the protonic conductivity of the membrane [11,12], increasing the electrical resistance of the fuel cell. This in turn reduces the fuel cell efficiency and can cause even more heating. In addition to this, excess heat can also cause a drying of the membrane which can lead to gas permeability, see Fig. 2.

Gas Diffusion Layer (GDL) degradation

The gas diffusion layer is usually made of the same or similar materials to the catalyst support and therefore many of the same degradation methods apply. Due to the lack of presence of the catalyst however, many of these methods occur at a slower rate in the GDL and therefore the GDL is the least studied MEA component [11,53]. Fuel starvation can cause oxidation of the carbon [11,12]. As with the catalyst layer, this may be due to insufficient fuel supply at high current densities or due to localised starvation during start/stop cycling or transient loading. The GDL is also susceptible to thermal and humidity management issues in a similar way to the membrane. Excess humidity at high current densities can cause flooding [12] leading to poor reactant supply to localised areas of the fuel cell [63] and high temperatures can increase the rate of oxidation of the carbon.

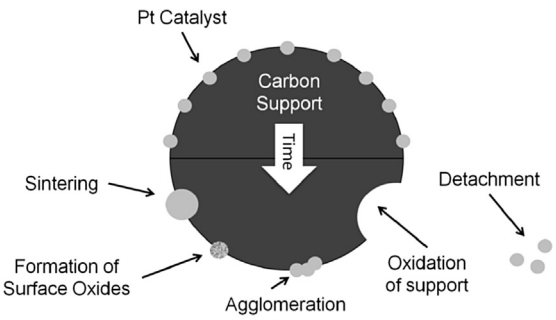

Fig. 1 – Diagram showing major causes of Electro-Chemical Active Surface Area (ECASA) reduction.

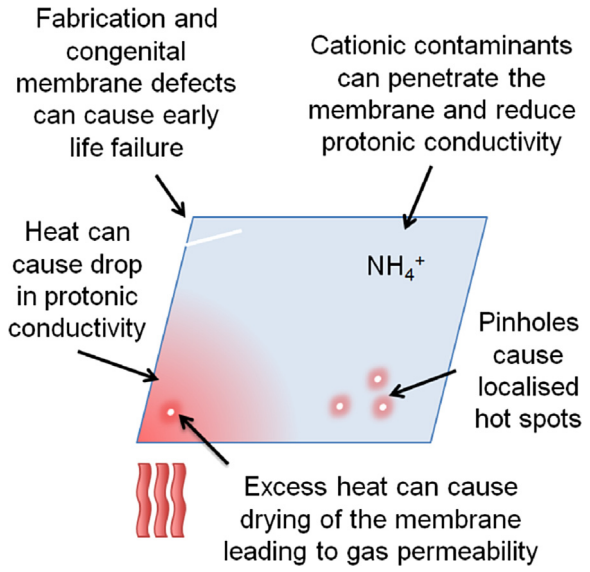

Fig. 2 – Diagram showing major causes of membrane degradation.

Generalised EMS targets

It can be seen that a number of these degradation methods are either directly or indirectly affected by decisions made by the EMS. It therefore makes sense to summarise the potential actions that the EMS can take in order to maximise the lifetime of the fuel cell;

1. Avoid running at very low current demands in order to limit ECASA reduction due to the formation of surface oxides on the catalyst [11,12,62,64].
2. Ensure current demand does not exceed reactant supply limitations to prevent both reactant starvation, which can lead to ECASA reduction, and excessive temperatures, which can lead to damage to the cathode support and to drying of the membrane [11,12,55].
3. Avoid excessive transient loading to maintain stable temperature and humidity in the fuel cell and prevent localised fuel starvation [12,54].
4. Limit start-up/shut-down cycling where possible to prevent non-uniform distribution of fuel and hence localised starvation [11,12,53,61,64].

These targets can be quantified as function that predicts the expected degradation due to each method, and hence used in the cost function for optimisation. Combined with the fuel consumption calculation and the predicted cost of the fuel cell, SDP can be used to minimise the overall running cost of the fuel cell.

Modelling

The vehicle used for testing is the Microcab H4, which is a low speed, low cost vehicle designed specifically for transporting passengers and mail on a university campus. The vehicle is configured as a series hybrid with a single brushed DC motor powering the rear wheels. The motor's electrical power is supplied by a nominal 48 V battery and a 24 V nominal fuel cell system is connected to the battery via a controllable DC/DC converter. More information about the design of the vehicle can be found in the following work by Kendall [65]. From more than two years of testing and over 4000 km of usage at the University of Birmingham, it has been found [57,66,67] that the 1.2 kW fuel cell system is unable to maintain the battery state of charge for sustained periods of driving. This meant that the fuel cell system was required to continue to run for up to 10 min after the vehicle was stopped at the end of each journey in order to recharge the battery. It is therefore desirable to examine the effects of fitting the vehicle with a larger 4.8 kW fuel cell system, which now exceeds the average power requirement of typical campus usage patterns. The full specification of the vehicle can be found in Table 1.

Vehicle model

The vehicle model used for the SDP optimisation needs to be iterated hundreds of thousands of times. Therefore it is imperative to keep the model as simple as possible in order to minimise computational time whilst still accurately replicating the vehicles behaviour. For this reason, a rearward facing model has been chosen. The information flow through the model can be seen in Fig. 3. It should be noted that most of the calculations are uni-directional and do not include any feedback loops aside from the battery voltage and power demand from the EMS. This also allows the model to be iterated very quickly in order to obtain the probability and cost matrices required for SDP optimisation.

The drag force on the vehicle is calculated using the standard straight-line performance Eq. (1), and this is combined with the inertial forces due to acceleration to calculate the total tractive effort (2).

$$F_D = \frac{1}{2}\rho C_d A v^2 - mg(A_d + B_d v) - B_{dem} - mg\sin(\beta) \quad (1)$$

$$F_{veh} = F_D + m_e\frac{dv}{dt} \quad (2)$$

The test vehicle uses a single fixed gear ratio to drive the rear wheels and therefore the motor speed, ω_{mot}, and torque, T_{mot}, can be easily calculated using the gear ratio, R_g and the rolling radius of the wheel, r_r (3, 4).

$$T_{mot} = F_{veh}\frac{r_r}{R_g} \quad (3)$$

Table 1 – Vehicle specification.

Characteristic	Value
Gross weight	940 kg
Traction motor type	Brushed DC
Traction motor peak power	12 kW
Fuel cell type	PEM
Fuel cell nominal power	4.8 kW
Traction battery type	Lead acid
Traction battery nominal capacity	2 kWh

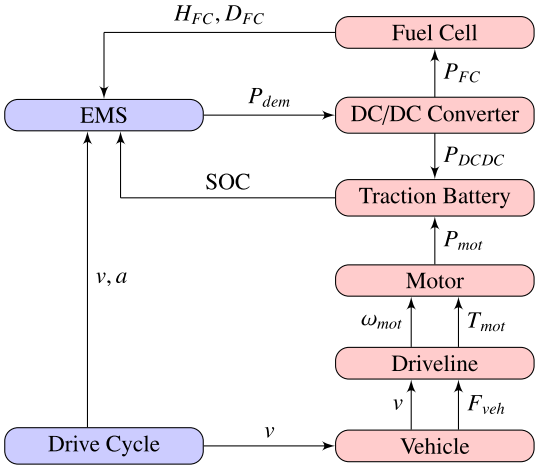

Fig. 3 – Vehicle model logic flow.

$$\omega_{mot} = v\frac{R_g}{r_r} \tag{4}$$

In order to maintain the simplicity of the model, the electrical power requirement of the electric motor, $P_{mot,elec}$, is calculated using empirical data obtained during chassis dynamometer testing. This model includes the efficiency of the motor, the mechanical driveline and power electronics required to drive the traction motor.

$$P_{mot,elec} = f(T_{mot}, \omega_{mot}) \tag{5}$$

The DC/DC converter output power, P_{DCDC}, is controlled directly by the EMS (6). The input power P_{FC} from the fuel cell can then be calculated using the output power and the DC/DC converter efficiency obtained from empirical data, η_{DCDC} (7).

$$P_{DCDC} = P_{dem} \tag{6}$$

$$P_{FC} = \frac{P_{DCDC}}{\eta_{DCDC}(P_{DCDC})} \tag{7}$$

The battery current, I_{bat}, is calculated using the power from the DC/DC converter and the motor, divided by the battery voltage, V_{bat} (8). The battery voltage itself is generated using a quasi-steady state combined Peukert-Shepherd model based on an averaged net current and the battery SoC (9), which is in turn calculated as the integral of the net battery current over time (10).

$$I_{bat} = \frac{P_{DCDC} - P_{mot,elec}}{V_{Bat}} \tag{8}$$

$$V_{bat} = f(I_{bat}, SoC) \tag{9}$$

$$SoC = \int I_{bat} \tag{10}$$

Finally, the fuel cell model uses empirical data to calculate the voltage, hydrogen consumption H_{FC}, and degradation, D_{FC}. The fuel consumption is simply calculated as a function of the fuel cell power (11). This data has been obtained from the equipment data-sheet and verified through preliminary testing of the vehicle.

$$H_{FC} = f(P_{FC}) \tag{11}$$

The ageing of the fuel cell is harder to quantify. From Section Generalised EMS targets, it can be seen that there are four main areas of interest with respect to the operating condition of the fuel cell; low power operation, high power operation, transient loading and start-stop cycles. Degradation due to operation at low and high current densities can be included as a function of the fuel cell operating power in a similar manner to the fuel consumption (12), where D_{power} is in the range $0 \leq D_{power} \leq 1$, representing proportion of degradation seen before the fuel cell requires replacement.

$$D_{power} = f(P_{FC}) \tag{12}$$

The degradation due to transient operation can be included in a similar manner where the degradation is instead proportional to the rate of change of fuel cell power (13).

$$D_{transients} = f\left(\frac{dP_{FC}}{dt}\right) \tag{13}$$

Finally, testing by the fuel cell manufacturer specifies a maximum number of start/stop cycles, n_{max}. The model allows for the fuel cell to be shut-down if the requested power is negative. This allows the proportional degradation due to a single shut-down to be calculated (14)

$$D_{cycle} = \begin{cases} \frac{1}{n_{max}}, & \text{if } P_{FC,t+1} \geq 0 \wedge P_{FC,t} < 0 \\ 0, & \text{otherwise} \end{cases} \tag{14}$$

Each of these degradation metrics represents the proportion of performance drop due to that method, where a fixed performance drop at nominal operating power represents end of life of the fuel cell stack. If the degradation methods are assumed to be largely independent, this allows the degradation due to each method to be summed together to obtain the total performance degradation of the fuel cell (15).

$$D_{FC} = D_{power} + D_{transients} + D_{cycle} \tag{15}$$

Cost function

The objective of the SDP optimisation is to choose actions in order to minimise a future anticipated cost. This cost is calculated by the use of a cost function. In order to minimise the total running cost of the fuel cell, the cost function should include not only the fuel consumption, but also the degradation of the fuel cell.

Ideally, the voltage degradation rate under each operating condition should be quantified by extensive testing of individual fuel cells; however, this would be extremely time-consuming and therefore has been deemed out of the scope of this work. Fortunately, there is enough data available in the manufacturer's data-sheet and previous literature [8], to make a reasonable estimate. The manufacturer states an expected degradation rate of approximately 11.6 μV/h per cell for the stack at full load, with essentially no degradation at part load (below approximately 80% full load). No idle degradation rates are given, however these have been obtained from the

literature for a similar fuel cell and scaled to match the full load data given by the manufacturer. An estimate for the voltage degradation has also been obtained from the literature, and the stop-start cycle voltage degradation has been obtained from the manufacturer's specification. These figures are given in Table 2.

In addition to minimising the total running cost of the fuel cell, the EMS is also responsible for managing the battery. This can be accomplished by setting constraints on the battery voltage which will prevent the battery from becoming over-charged or deeply discharged. By using the battery voltage, rather than state of charge directly, the battery will also be protected from voltage spikes during regenerative braking and from voltage drops during periods of high current demand, such as acceleration. This has been achieved by assigning a cost to extreme cell potentials (V_{max} and V_{min}), see Eq. (16).

$$C_V = \begin{cases} \int (V_{min} - V_{bat})dt, & \text{if } V_{bat} < V_{min} \\ \int (V_{bat} - V_{max})dt, & \text{if } V_{bat} > V_{max} \\ 0, & \text{otherwise} \end{cases} \quad (16)$$

The final cost function (17) is made up by weighting and summing the individual costs of the fuel, the fuel cell degradation and the battery voltage constraints. The fuel and fuel cell are weighted by their respective monetary values, V_{fuel} and V_{FC}, in order to estimate the total running cost of the fuel cell. By assigning a very high penalty cost to the voltage weighting parameter, α; it acts as a "soft" constraint on the optimisation, effectively preventing the resulting strategy from running in conditions that are likely to severely damage the battery. The exact numerical value of this is not important; however it should be orders of magnitude higher than the values to be optimised.

$$C_{total} = -\left(H_{FC}V_{fuel} + D_{FC}V_{FC} + \alpha C_V\right) \quad (17)$$

Drivecycle model

The SDP problem formulation requires the input of a stochastic model of the duty cycle that the vehicle is likely to face. Obviously, the accuracy of this model has a significant contribution on the quality of the results and therefore in order to populate this model, real-world logged data of the vehicle has been used. These data were collected between 2008 and 2009 by Iain Staffell et al. [67] on the University of Birmingham campus whilst the vehicle was used for passenger transport and mail delivery. For the purposes of this analysis, the gradient of the road has been ignored, but for real world use, this would need to be included because it could significantly affect the results. These data were used to create a first order Markov Chain model, see Eq. (18), Fig. 4.

$$p_{ijm} = \Pr(a_{k+1} = j | a_k = i, v_k = m) \quad (18)$$

Table 2 – PEM fuel cell degradation rates (per cell).

Operating conditions	Degradation rate
Low power operation	10.17 μV/h
High power operation	11.74 μV/h
Transient loading	0.0441 μV/Δkw
Start/stop	23.91 μV/cycle

Methodology

Markov Decision Process (MDP) problem

A MDP problem can be defined by a set of decision epochs, T, a set of Actions, A_s, a set of States, S, the probabilities of transitioning between each state, $P_{a,ij}$, and the reward or cost of each transition $C_{a,ij}$. The sample rate of the logged data is 1 s, and this is acceptable to use for the MDP problem, any dynamic effects greater than this can be reasonably ignored (19). For design of an EMS for a FCHEV, the set of actions must determine the operating point of either the battery pack or the fuel cell and therefore the output power of the main DC/DC converter has been chosen (20) as this is proportional to the fuel cell power.

$$T = \{0, 1, \ldots\}\text{s} \quad (19)$$

$$A_s = P_{FC} = \{0, \ldots, P_{max}\}\text{W} \quad (20)$$

The number of states in the problem significantly affects the computational burden, but must be sufficient to allow accurate calculation of the cost function. Firstly, the speed and acceleration of the vehicle determine the electrical power consumption of the motor and therefore they must be included. The battery SoC must also be included in order to constrain the SoC within acceptable limits and protect the battery. Finally, the fuel cell power is also included in order to penalise excessive load cycling and high rate of power demand transitions.

$$S = S(a, v, \text{SoC}, P_{FC}) \quad (21)$$

The probability and cost matrices are generated using the vehicle model by simulating every valid action from every

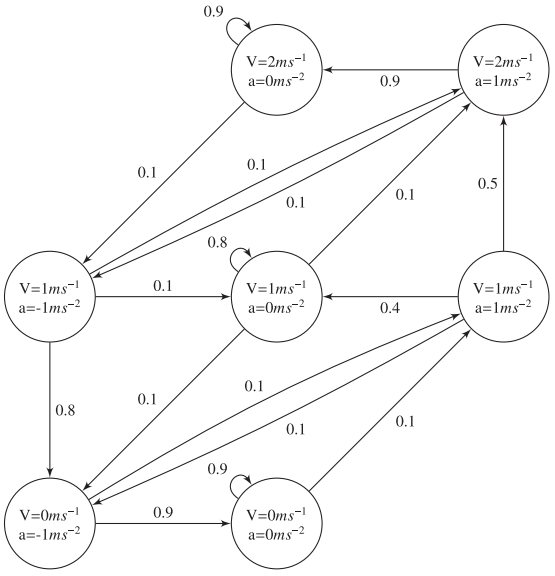

Fig. 4 – Example Markov Chain Drivecycle model.

initial state. The subsequent state and associated cost of performing each action from each initial state is calculated from the simulation results. The cost is easily calculated using the cost function, however, the subsequent state may not match one of the finite states in the MDP problem. The problem arises that some actions will result in movement of only a tiny fraction of the grid spacing. This is most apparent with the battery SoC which hardly changes over the time-step of one second and it would be infeasible to reduce the grid spacing enough. In order to alleviate this problem, the subsequent state is represented by a probability distribution split between the grid points. This probability distribution is multiplied by that of the Markov model in order to generate the full transitional probability matrix (see Fig. 5).

Stochastic Dynamic Programming (SDP) solution

The MDP problem described is solved using SDP. The objective is to find the optimal control policy, $u = \pi^*(S)$ so as to minimise the total expected cost, $J_\pi(S_0)$, over an infinite horizon. The total expected cost is calculated using (22), where $\alpha \in [0, 1)$, represents the one second discount factor.

$$J_\pi(S_0) = \lim_{T\to\infty} E\left\{\sum_{t=0}^{T-1} \alpha^{t-1} C(S_t, \pi(S_t))\right\} \quad (22)$$

The optimal policy can be found using a policy iteration algorithm. This works by iteratively evaluating the current policy and then improving the policy until the policy converges. The policy evaluation step (23), given the current control policy, π is calculated as the cost incurred during the current step added to the expected cost of future steps given the new state, S', that the vehicle has transitioned to.

$$J_\pi^{t+1}(S^i) = C(S^i, \pi(S^i)) + \alpha E\{J_\pi^t(S')\} \quad (23)$$

The policy is then improved by finding the action which will minimise the total expected cost (24).

$$\pi'(x') = \arg\min_{a\in A(S^i)} \left[C(S^i, a) + \alpha E\{J_\pi(x')\}\right] \quad (24)$$

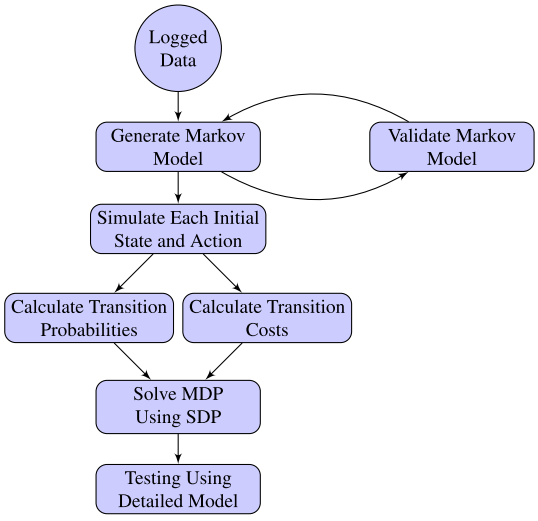

Fig. 5 – Flowchart of the procedure used to generate a real-time controller.

This process is iterated until the policy remains unchanged for a number of improvement steps. The optimal policy $\pi^*(S)$ will be based on the state of the vehicle, causal and time-invariant and therefore can be directly implemented in simulation or on-board the vehicle.

The SDP algorithm was iterated with 100 policy evaluation steps for each improvement step and was deemed to be converged when the policy remained unchanged for 36 improvement steps, representing approximately one hour drive time. This combination was found to be the most time effective in order to produce reliable results. A value of α of 0.9999 was chosen for the one second discount factor. This value is relatively high compared to what is found in the literature (0.95–0.995) [33,34,41,42], however this was found to be required for charge sustaining behaviour in the long term when using only the battery voltage to constrain the SoC. Using these settings, the SDP optimisation took approximately 6 h to solve on a desktop PC using a 3.5 GHz quad-core processor.

Results

The result of the SDP algorithm is a multi-dimensional lookup table which outputs the optimal control action for each possible vehicle state. This look-up table can be directly implemented in the simulation model and run in real time. The controller optimised for degradation has been compared to a baseline controller which is optimised purely on the fuel consumption.

An example set of results is shown in for the baseline controller is shown in Fig. 6a and for the degradation optimised controller in Fig. 6b. This data-set assumes a fuel cost of £1.99/kg ($2.87/kg) of hydrogen and a fuel cell cost of £33.22/kW ($47.97/kW). These results show the response of the two controllers over a low speed, stop-start duty cycle typical for the test vehicle. It can be seen from the speed trace at the top of each figure that the drive-cycle is split into four discrete journey's, lasting approximately 5–10 min each and taking place over almost one hour. The maximum speed is 6.9 m/s and the peak tractive power is 4.93 kW. For each test, the battery SoC has been initialised so that there is minimal net change over the complete journey. This avoids any complications involved with accounting for energy stored in the battery and also allows the typical SoC range of each strategy to be examined. Other than this, the input to each controller is identical.

For the baseline strategy (Fig. 6a), the total anticipated cost for this journey is £0.28, with £0.11 (40%) due to fuel consumption and £0.17 due to degradation of the fuel cell. Approximately three quarters of cost of the degradation (£0.13) in the baseline strategy is simply the cost of the single on/off cycle. Of the remaining degradation cost, approximately half is due to the fuel cell idling for long periods in between the journeys, and half of the cost occurs due to the highly transient loading on the fuel cell in response to the current drawn by the motor.

In comparison, the total estimated journey cost for the degradation optimised controller is around £0.26, of which approximately 45% is due to the cost of the fuel used.

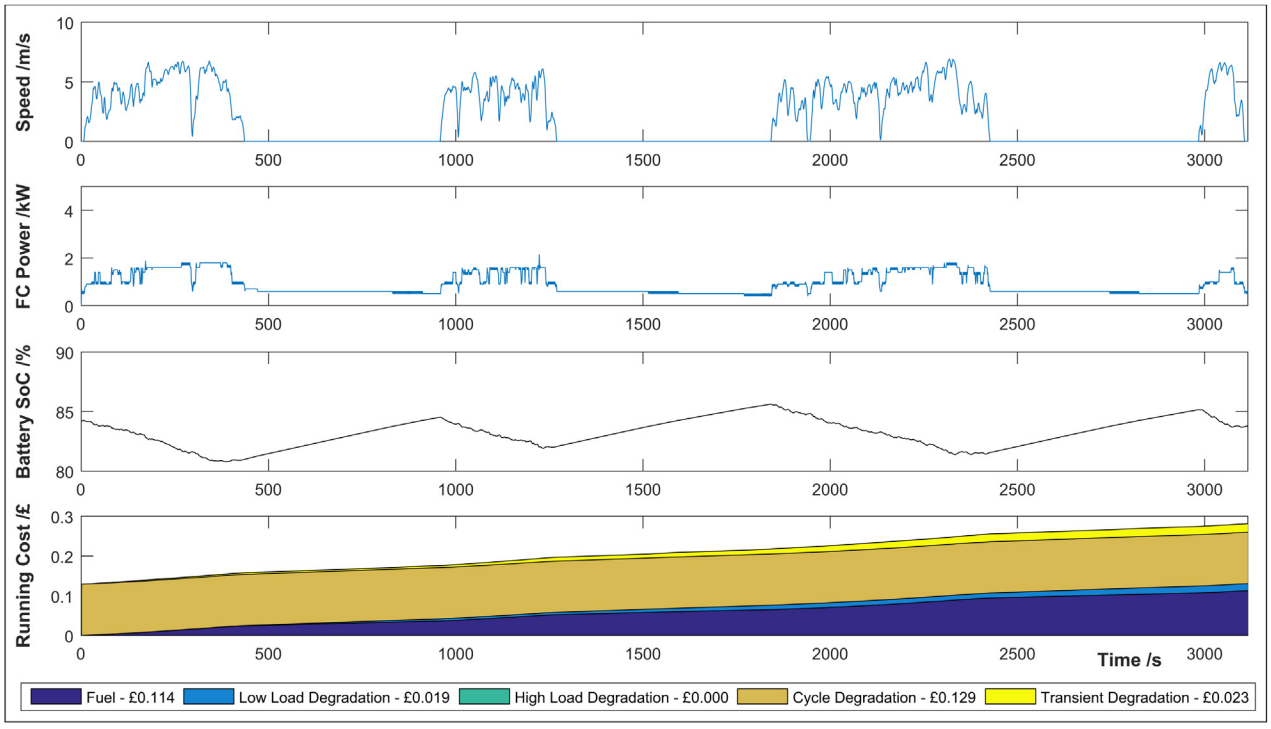

(a) Baseline Controller

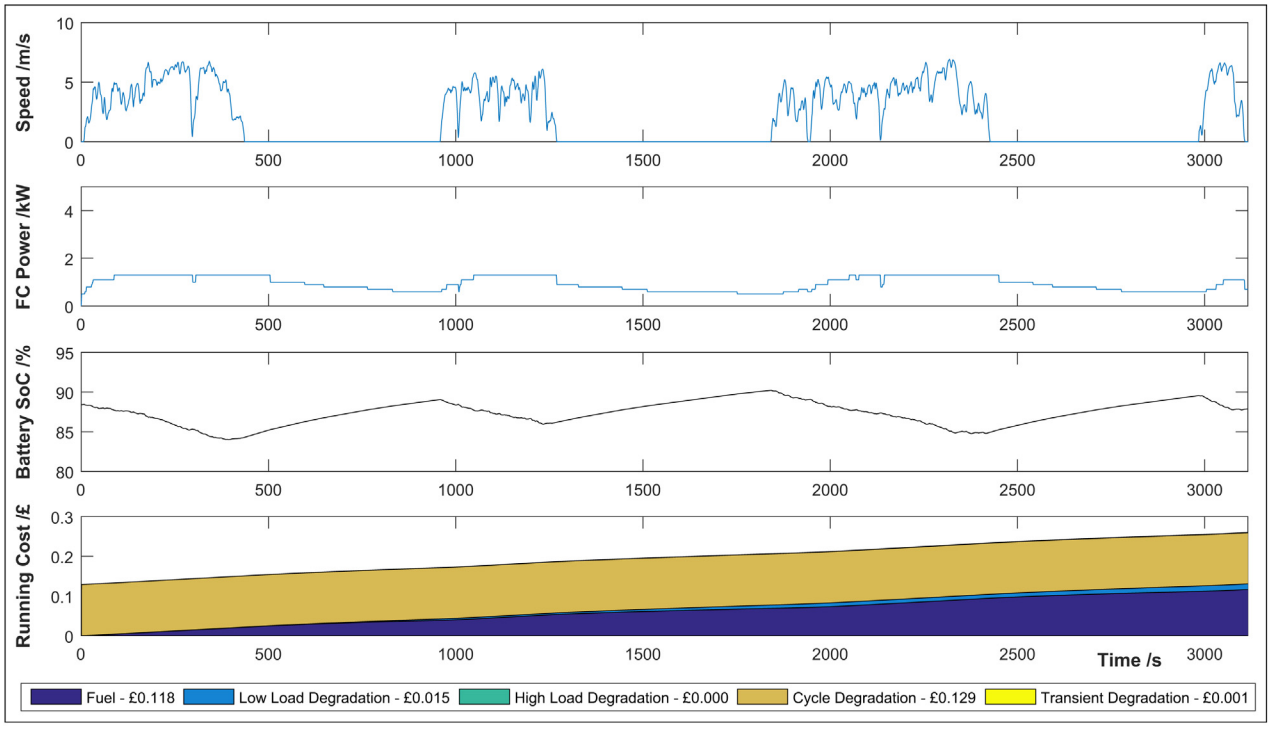

(b) Degradation Optimised Controller

Fig. 6 – Accumulated running cost of each controller.

Overall, the new strategy reduces the estimated degradation by 15% when compared to the baseline strategy. Again, the overwhelming majority (89%) of the degradation is due to the single start/stop cycle of the fuel cell, however there is a significant reduction (97%) in the transient loading on the fuel cell, and degradation due to low power operation is also reduced by approximately 21%. The fuel consumption for the new strategy has only been increased by 3.6% resulting in an overall cost saving of 7.6% for the drive-cycle.

Discussion

Battery SoC sustenance

As previously mentioned, the initial battery SoC has been chosen individually for each test so that minimal net change is observed over the cycle. It can be seen that each controller has been initialised with a different value. The reason for this is that charge sustenance is indirectly achieved by the battery voltage constraints. As result, there is no explicit target SoC value and each controller will find its own natural equilibrium in order to produce the desired charge sustaining behaviour.

It can be seen in Fig. 6a that the baseline controller tends to respond very quickly to the instantaneous electric load from the motors and, as a result, maintains a relatively consistent battery SoC. In contrast, the degradation optimised strategy tends to run at a more consistent fuel cell load, resulting in much more deviation of the battery SoC over the duty cycle. This minimises the transient loading on the fuel cell in order to prevent degradation, and also limits the time that the fuel cell is idling, and therefore also reduces degradation due to low power operation.

The two strategies perform slightly differently with regards to the overall battery SoC. The degradation optimised strategy maintains a slightly higher SoC on the battery (84–90%) compared to the baseline strategy (82–87%). This is likely due to the fact that the new strategy is penalised for transient loading and is therefore less inclined to respond quickly to sudden load changes. By running at a higher overall SoC, it is less likely to allow the battery voltage to drop below the minimum constraint given it's slower response. Conversely, the baseline strategy is not penalised for sudden load changes, and therefore runs closer to the minimum acceptable voltage in order to conserve fuel in the short term.

Degradation cost saving vs fuel consumption

Fig. 7 shows the results of simulations of both controllers over 10 logged drive-cycles. The LHS bar of each group represents the baseline controller and the RHS bar represents the controller optimised to minimise degradation. It can be seen that the overall running cost for the new controller is much lower in every case due to the reduction in the estimated degradation, despite a marginal increase in fuel consumption for each of a logged journeys.

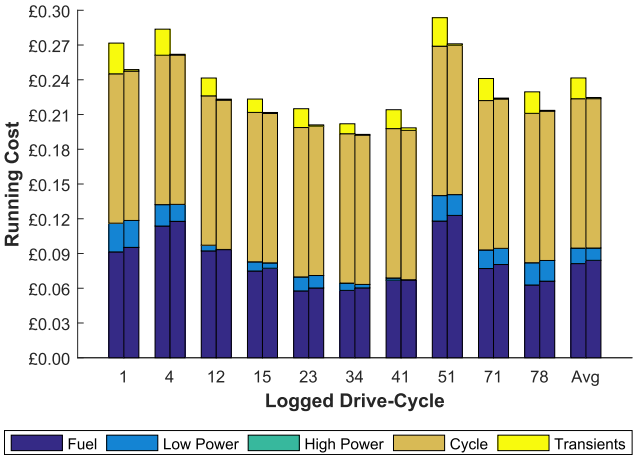

Fig. 7 – Cost reduction due to reduced degradation.

The baseline controller represents the ideal management strategy for minimising the fuel consumption and therefore the new strategy is expected to increase the fuel consumption. However, it can be seen in Fig. 7 that this effect is minimal when compared to the reduction in degradation. The average fuel consumption for the baseline controller was 10.2 g/km and for the degradation inclusive strategy it was 10.5 g/km. The inclusion of the degradation optimisation results in a fuel consumption increase of between 0.5 and 5.3% (averaging 3.5%) over the duty cycles tested. This is likely due to the fact that the ideal operating points for minimising fuel consumption and minimising degradation largely coincide at approximately 30–50% maximum power. Therefore it is only when attempting to minimise transient loading where the degradation cost is likely to compete with the fuel cost.

The new strategy results in an average of 12.3% reduction in cost associated with degradation, resulting in an overall 7% reduction in the estimated running cost. The vast majority of this cost saving is due to the reduction in the transient loading on the fuel cell by approximately 94%, but there is also a 20.5% reduction in degradation due to reduced operation at low power. Both controllers are assumed to keep the fuel cell running for the entire duration of the drive-cycle, and therefore both saw the same degradation cost due to start-stop cycling which represented a large proportion of the total degradation in each drive-cycle, especially for the optimised controller. Neither controller operated the fuel cell above 80% peak power, therefore no degradation was seen due to high power in either case.

Operating lifetime

This 12% reduction in degradation results in a 14% increase in the estimated fuel cell lifetime, from 616 h (averaged over 10 drive-cycles) for the baseline strategy to 702 h for the degradation optimised strategy. This is still significantly below the US DoE target of 5000 h, however approximately 92% of the degradation observed is due to the unavoidable cost of a single start-stop cycle for each journey. In fact, considerable variation in this estimate was observed over the 10 duty cycles tested, which can be seen in Fig. 8. This variation is approximately inversely correlated to the length of the duty cycle and is due to the fact that the single on/off cycle causes proportionally more degradation for shorter journeys.

The fuel cell used in the Microcab shows a rate of degradation due to start-stop cycling of approximately 23.91 μV/cycle/cell. This means that even with no degradation from other methods, the fuel cell would only last approximately 1200 cycles before being considered at the end of its useful life. As the drive-cycle lengths average approximately 37 min, this represents a theoretical maximum of lifetime of only 750 h if no degradation was seen due to other causes. The baseline controller results in a deficit of 134 h compared to this figure, whereas the new controller reduces this deficit by 64% to just 48 h by minimising the voltage degradation due to other causes.

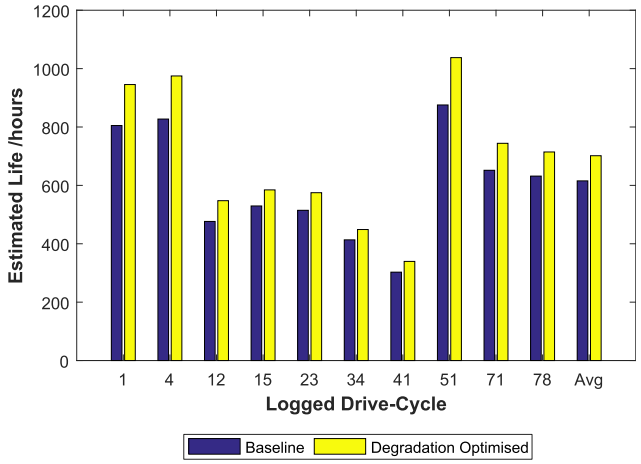

Fig. 8 – Estimated fuel cell lifetime.

In comparison to a more recent fuel cell used by Chen et al. [8], the fuel cell in the Microcab exhibits quite high degradation due to cycling. Chen et al. used a figure of 13.79 μV/cycle/cell. If this number were to be used instead of that from the Ballard datasheet, the degradation due to cycling would still represent approximately 70% for the baseline controller and 86% for the degradation optimised controller. This increases the predicted lifetime of the fuel cell to 934 h for the baseline controller and 1147 h for the optimised controller. In this case the lifetime of the fuel cell has been increased by 23% due to the optimised control; however it is still well below the US DoE target for vehicular applications.

Overall, optimisation of the degradation results in a statistically significant increase in the estimated fuel cell lifetime. It does this by significantly reducing the degradation due to transient loading and due to operation at idle loading; however the degradation due to start-stop cycling limits its potential. This suggests that this could be an important area of focus for future fuel cell stack design. Finally, it must be noted that the model assumes that each degradation method for the fuel cell occurs linearly with time and is independent of other methods. This assumption may be valid in the short-term, however in the long term; this may not be the case so estimates of the prediction of overall lifetime may not be as accurate as that of the short term degradation.

Conclusions

Due to the high cost of a fuel cell system and its relatively low durability compared to conventional powertrains, it is important to maximise the lifetime of the stack on board any FCHEV. By including the expected degradation in the cost function when using optimal control for the EMS, it is possible to dramatically reduce the degradation due to EMS decisions. This results in a significant (12.3%) reduction in the cost due to fuel cell degradation and an estimated increase in lifetime of the stack of 14%.

The optimised controller works by significantly reducing the transient loading on the fuel cell, tending to run at an overall average power demand and allowing the battery SoC to reduce during periods of high demand and re-charge while the vehicle is stationary. This also reduces the time that the fuel cell is running at an idle load. The fuel cell in the Microcab exhibits relatively high degradation due to start-stop cycling, of which the SDP controller can do very little about, and therefore this method dominates the other degradation causes for the optimised controller. For a fuel cell stack design which is more tolerant of start-stop cycling the potential for increasing the operating lifetime is further improved.

The fuel consumption of the vehicle is largely unaffected (3.5%) by this inclusion due to the fact that the optimal operating points for reliability and fuel efficiency largely coincide. As a result, the overall running cost is reduced by approximately 7%.

Further work

It must be noted that this analysis does not take into account any damage that may be done to the batteries in absorbing these transient loads. For the Microcab H4, this fact is relatively negligible due to the low cost and high durability of the lead acid battery pack, but for lithium based batteries used on many hybrid vehicles, the anticipated increase in degradation cost of the batteries may be significant.

Increasing the fuel cell stack size from 1.2 kW to 4.8 kW allowed the controller to effectively manage the fuel consumption and fuel cell degradation when compared to previous work [57]. However, it has been noted that the fuel cell stack was not run near the high power degradation region by either of the two controllers developed in this analysis. This may suggest that a 4.8 kW system may be slightly oversized for the duty cycle experienced on campus. Therefore, it may be interesting to compare the results of the SDP algorithm for different sized stacks and battery packs in order to further minimise the overall lifetime cost of the vehicle.

A further extension of both of these ideas would be to include supercapacitors in the system in order to absorb some of the transient loading and protect both the fuel cell and battery pack. The increased cost and complexity of the system could then be directly compared to the anticipated financial benefit of extending the lifetime of the other components.

Acknowledgements

The authors would like to acknowledge Dr. Iain Staffell for providing the logged data of the test vehicles from their use on the University of Birmingham campus in order to build the stochastic drive-cycle model, Microcab Ltd. for providing the test vehicle itself, and the EPSRC for providing funding for the project through the Doctoral Training Centre in Hydrogen, Fuel Cells and Their Applications (EP/G037116/1), access to the underlying data will be made available at https://lboro.figshare.com/.

Acronyms

DDP	Deterministic Dynamic Programming
DoE	Department of Energy
ECASA	Electro-Chemical Active Surface Area
ECMS	Equivalent Consumption Minimization Strategy
EMS	Energy Management Strategy
EPSRC	Engineering and Physical Sciences Research Council
FCHEV	Fuel Cell Hybrid Electric Vehicle
GDL	Gas Diffusion Layer
HEV	Hybrid Electric Vehicle
ICE	Internal Combustion Engine
MDP	Markov Decision Process
MEA	Membrane Electrode Assembly
PEM	Proton Exchange Membrane
SDP	Stochastic Dynamic Programming
SoC	State of Charge

REFERENCES

[1] Lin C-C, Peng H, Grizzle JW, Liu J, Busdiecker M. Control system development for an advanced-technology medium-duty hybrid electric truck. Tech. Rep. 2003-01-3369. SAE, 2003. http://dx.doi.org/10.4271/2003-01-3369.

[2] Kim M, Sohn Y-J, Lee W-Y, Kim C-S. Fuzzy control based engine sizing optimization for a fuel cell/battery hybrid mini-bus. J Power Sources 2008;178(2):706–10. http://dx.doi.org/10.1016/j.jpowsour.2007.12.047.

[3] Ansarey M, Panahi MS, Ziarati H, Mahjoob M. Optimal energy management in a dual-storage fuel-cell hybrid vehicle using multi-dimensional dynamic programming. J Power Sources 2014;250:359–71. http://dx.doi.org/10.1016/j.jpowsour.2013.10.145.

[4] Pisu P, Rizzoni G. A comparative study of supervisory control strategies for hybrid electric vehicles. Control Syst Technol IEEE Trans 2007;15(3):506–18. http://dx.doi.org/10.1109/TCST.2007.894649.

[5] Vidal-Naquet F, Zito G. Adapted optimal energy management strategy for drivability. In: Vehicle Power and Propulsion Conference (VPPC), 2012 IEEE; 2012. p. 358–63. http://dx.doi.org/10.1109/VPPC.2012.6422678.

[6] Opila D, Wang X, McGee R, Gillespie R, Cook J, Grizzle J. An energy management controller to optimally trade off fuel economy and drivability for hybrid vehicles. IEEE Trans Control Syst Technol 2012;20(6):1490–505. http://dx.doi.org/10.1109/TCST.2011.2168820.

[7] Rousseau A, Sharer P, Ahluwalia R. Energy storage requirements for fuel cell vehicles. Tech. Rep. 2004-01-1302. SAE, 2004. http://dx.doi.org/10.4271/2004-01-1302.

[8] Chen H, Pei P, Song M. Lifetime prediction and the economic lifetime of proton exchange membrane fuel cells. Appl Energy 2015;142:154–63. http://dx.doi.org/10.1016/j.apenergy.2014.12.062.

[9] Dresselhaus M, Crabtree G, Buchanan M, Basic research needs for the hydrogen economy: report on the basic energy sciences workshop on hydrogen production, storage, and use, Office of Science, US Department of Energy.

[10] Borup R, Meyers J, Pivovar B, Kim YS, Mukundan R, Garland N, et al. Scientific aspects of polymer electrolyte fuel cell durability and degradation. Chem Rev 2007;107(10):3904–51. http://dx.doi.org/10.1021/cr050182l.

[11] Yuan X-Z, Li H, Zhang S, Martin J, Wang H. A review of polymer electrolyte membrane fuel cell durability test protocols. J Power Sources 2011;196(22):9107–16. http://dx.doi.org/10.1016/j.jpowsour.2011.07.082.

[12] Placca L, Kouta R. Fault tree analysis for PEM fuel cell degradation process modelling. Int J Hydrogen Energy 2011;36(19):12393–405. http://dx.doi.org/10.1016/j.ijhydene.2011.06.093.

[13] Sciarretta A, Guzzella L. Control of hybrid electric vehicles: optimal energy management strategies. IEEE Control Syst 2007;27(2):60–70. http://dx.doi.org/10.1109/MCS.2007.338280.

[14] Schell A, Peng H, Tran D, Stamos E, Lin C-C, Kim MJ. Modelling and control strategy development for fuel cell electric vehicles. Annu Rev Control 2005;29(1):159–68. http://dx.doi.org/10.1016/j.arcontrol.2005.02.001.

[15] Bauman J, Kazerani M. A comparative study of fuel-cell-battery, fuel-cell-ultracapacitor, and fuel-cell-battery-ultracapacitor vehicles. IEEE Trans Veh Technol 2008;57(2):760–9. http://dx.doi.org/10.1109/TVT.2007.906379.

[16] Xiong W-w, Zhang Y, Yin C-l. Configuration design, energy management and experimental validation of a novel series-parallel hybrid electric transit bus. J Zhejiang Univ Sci A 2009;10:1269–76. http://dx.doi.org/10.1631/jzus.A0820556.

[17] Schaltz E, Khaligh A, Rasmussen P. Influence of battery/ultracapacitor energy-storage sizing on battery lifetime in a fuel cell hybrid electric vehicle. IEEE Trans Veh Technol 2009;58(8):3882–91. http://dx.doi.org/10.1109/TVT.2009.2027909.

[18] Harmon FG, Frank AA, Joshi SS. The control of a parallel hybrid-electric propulsion system for a small unmanned aerial vehicle using a CMAC neural network. Neural Netw 2005;18(56):772–80. http://dx.doi.org/10.1016/j.neunet.2005.06.030.

[19] Dextreit C, Kolmanovsky IV. Game theory controller for hybrid electric vehicles. IEEE Trans Control Syst Technol 2013;22(99):652–63. http://dx.doi.org/10.1109/TCST.2013.2254597.

[20] Brahma A, Guezennec Y, Rizzoni G. Optimal energy management in series hybrid electric vehicles. In: Proceedings of the 2000 American Control Conference, no. 6 in 2000 American Control Conference; 2000. p. 60–4. http://dx.doi.org/10.1109/ACC.2000.878772.

[21] Lin C-C, Peng H, Grizzle J, Kang J-M. Power management strategy for a parallel hybrid electric truck. IEEE Trans Control Syst Technol 2003;11(6):839–49. http://dx.doi.org/10.1109/TCST.2003.815606.

[22] Fares D, Chedid R, Panik F, Karaki S, Jabr R. Dynamic programming technique for optimizing fuel cell hybrid vehicles. Int J Hydrogen Energy 2015;40(24):7777–90. http://dx.doi.org/10.1016/j.ijhydene.2014.12.120. hydrogen and Fuel Cell Systems for Clean Energy Applications.

[23] Johnson VH, Wipke KB, Rausen DJ. Hev control strategy for real-time optimization of fuel economy and emissions. Tech. Rep. 2000-01-1543. SAE; 2000.

[24] Paganelli G, Tateno M, Brahma A, Rizzoni G, Guezennec Y. Control development for a hybrid-electric sport-utility vehicle: strategy, implementation and field test results. In: American Control Conference, 2001. Proceedings of the 2001, vol. 6; 2001. p. 5064–9. http://dx.doi.org/10.1109/ACC.2001.945787.

[25] Guezennec Y, Choi T-Y, Paganelli G, Rizzoni G. Supervisory control of fuel cell vehicles and its link to overall system efficiency and low-level control requirements. In: American Control Conference, 2003. Proceedings of the 2003, vol. 3; 2003. p. 2055–61. http://dx.doi.org/10.1109/ACC.2003.1243377.

[26] Pisu P, Koprubasi K, Rizzoni G. Energy management and drivability control problems for hybrid electric vehicles. In: Decision and Control, 2005 and 2005 European Control

Conference. CDC-ECC '05. 44th IEEE Conference on; 2005. p. 1824–30. http://dx.doi.org/10.1109/CDC.2005.1582425.
[27] Musardo C, Rizzoni G, Guezennec Y, Staccia B. A-ECMS: an adaptive algorithm for hybrid electric vehicle energy management. Eur J Control 2005;11(4–5):509–24. http://dx.doi.org/10.3166/ejc.11.509-524.
[28] Zhang P-z, Yin C-l, Zhang Y, Wu Z-w. Optimal energy management for a complex hybrid electric vehicle: tolerating power-loss of motor. J Shanghai Jiaot Univ (Sci) 2009;14:476–81. http://dx.doi.org/10.1007/s12204-009-0476-6.
[29] Sinoquet D, Rousseau G, Milhau Y. Design optimization and optimal control for hybrid vehicles. Optim Eng 2011;12:199–213. http://dx.doi.org/10.1007/s11081-009-9100-8.
[30] Chasse A, Sciarretta A. Supervisory control of hybrid powertrains: an experimental benchmark of offline optimization and online energy management. Control Eng Pract 2011;19(11):1253–65. http://dx.doi.org/10.1016/j.conengprac.2011.04.008.
[31] Garcia P, Torreglosa J, Fernandez L, Jurado F. Viability study of a FC-battery-SC tramway controlled by equivalent consumption minimization strategy. Int J Hydrogen Energy 2012;37(11):9368–82. http://dx.doi.org/10.1016/j.ijhydene.2012.02.184.
[32] Vagg C. Optimal control of hybrid electric vehicles for real-world driving patterns. Ph.D. thesis, Department of Mechanical Engineering, University of Bath; 2014.
[33] Kolmanovsky I, Siverguina I, Lygoe B. Optimization of powertrain operating policy for feasibility assessment and calibration: stochastic dynamic programming approach. In: Proceedings of the 2002 American Control Conference, vol. 2; 2002. p. 1425–30. http://dx.doi.org/10.1109/ACC.2002.1023221.
[34] Lin C-C, Peng H, Grizzle J. A stochastic control strategy for hybrid electric vehicles. In: Proceedings of the 2004 American Control Conference, vol. 5; 2004. p. 4710–5.
[35] Lin C-C, Kim M-J, Peng H, Grizzle JW. System-level model and stochastic optimal control for a PEM fuel cell hybrid vehicle. J Dyn Syst Meas Control 2006;128(4):878–90. http://dx.doi.org/10.1115/1.2362785.
[36] Kim M-J, Peng H. Power management and design optimization of fuel cell/battery hybrid vehicles. J Power Sources 2007;165(2):819–32. http://dx.doi.org/10.1016/j.jpowsour.2006.12.038.
[37] Opila D, Aswani D, McGee R, Cook J, Grizzle J. Incorporating drivability metrics into optimal energy management strategies for hybrid vehicles. In: Decision and Control, 2008. CDC 2008. 47th IEEE Conference on; 2008. p. 4382–9. http://dx.doi.org/10.1109/CDC.2008.4738731.
[38] Moura S, Stein J, Fathy H. Battery-health conscious power management in plug-in hybrid electric vehicles via electrochemical modeling and stochastic control. Control Syst Technol IEEE Trans 2013;21(3):679–94. http://dx.doi.org/10.1109/TCST.2012.2189773.
[39] Zhang H, Qin Y, Li X, Liu X. Driver-oriented optimization of power management in plug-in hybrid electric vehicles. In: EIC Climate Change Technology Conference 2013, no. 1569730735 in CCTC 2013; 2013. p. 1–12.
[40] Vagg C, Akehurst S, Brace CJ, Ash L. Stochastic dynamic programming in the real-world control of hybrid electric vehicles. IEEE Trans Control Syst Technol 2016;PP(99):1–14. http://dx.doi.org/10.1109/TCST.2015.2498141.
[41] Johannesson L, Asbogard M, Egardt B. Assessing the potential of predictive control for hybrid vehicle powertrains using stochastic dynamic programming. IEEE Trans Intell Transp Syst 2007;8(1):71–83. http://dx.doi.org/10.1109/TITS.2006.884887.
[42] Tate ED, Grizzle JW, Peng H. Shortest path stochastic control for hybrid electric vehicles. Int J Robust Nonlinear Control 2008;18(14):1409–29. http://dx.doi.org/10.1002/rnc.1288.
[43] Schiffer J, Bohlen O, De Doncker R, Sauer D, Ahn KY. Optimized energy management for fuelcell-supercap hybrid electric vehicles. In: 2005 IEEE Conference Vehicle Power and Propulsion; 2005. p. 341–8. http://dx.doi.org/10.1109/VPPC.2005.1554637.
[44] Zheng C, Kim N, Cha S. Optimal control in the power management of fuel cell hybrid vehicles. Int J Hydrogen Energy 2012;37(1):655–63. http://dx.doi.org/10.1016/j.ijhydene.2011.09.091. 11th China Hydrogen Energy Conference.
[45] Xu L, Ouyang M, Li J, Yang F, Lu L, Hua J. Application of pontryagin's minimal principle to the energy management strategy of plugin fuel cell electric vehicles. Int J Hydrogen Energy 2013;38(24):10104–15. http://dx.doi.org/10.1016/j.ijhydene.2013.05.125.
[46] Thounthong P, Chunkag V, Sethakul P, Davat B, Hinaje M. Comparative study of fuel-cell vehicle hybridization with battery or supercapacitor storage device. IEEE Trans Veh Technol 2009;58(8):3892–904. http://dx.doi.org/10.1109/TVT.2009.2028571.
[47] Thounthong P, Ral S, Davat B. Energy management of fuel cell/battery/supercapacitor hybrid power source for vehicle applications. J Power Sources 2009;193(1):376–85. http://dx.doi.org/10.1016/j.jpowsour.2008.12.120.
[48] Aouzellag H, Ghedamsi K, Aouzellag D. Energy management and fault tolerant control strategies for fuel cell/ultra-capacitor hybrid electric vehicles to enhance autonomy, efficiency and life time of the fuel cell system. Int J Hydrogen Energy 2015;40(22):7204–13. http://dx.doi.org/10.1016/j.ijhydene.2015.03.132.
[49] Pukrushpan JT, Peng H, Stefanopoulou AG. Control-oriented modeling and analysis for automotive fuel cell systems. J Dyn Syst Meas Control 2004;126(1):14–25. http://dx.doi.org/10.1115/1.1648308.
[50] Vahidi A, Stefanopoulou A, Peng H. Current management in a hybrid fuel cell power system: a model-predictive control approach. IEEE Trans Control Syst Technol 2006;14(6):1047–57. http://dx.doi.org/10.1109/TCST.2006.880199.
[51] Xu L, Li J, Ouyang M, Hua J, Yang G. Multi-mode control strategy for fuel cell electric vehicles regarding fuel economy and durability. Int J Hydrogen Energy 2014;39(5):2374–89. http://dx.doi.org/10.1016/j.ijhydene.2013.11.133.
[52] Pukrushpan JT, Peng H, Stefanopoulou AG. Control of fuel cell power systems. Springer; 2008.
[53] Zhang S, Yuan X, Wang H, Mrida W, Zhu H, Shen J, et al. A review of accelerated stress tests of mea durability in PEM fuel cells. Int J Hydrogen Energy 2009;34(1):388–404. http://dx.doi.org/10.1016/j.ijhydene.2008.10.012.
[54] Liu D, Case S. Durability study of proton exchange membrane fuel cells under dynamic testing conditions with cyclic current profile. J Power Sources 2006;162(1):521–31. http://dx.doi.org/10.1016/j.jpowsour.2006.07.007.
[55] Sun J, Kolmanovsky I. Load governor for fuel cell oxygen starvation protection: a robust nonlinear reference governor approach. Control Syst Technol IEEE Trans 2005;13(6):911–20. http://dx.doi.org/10.1109/TCST.2005.854323.
[56] Pukrushpan J, Stefanopoulou A, Peng H. Control of fuel cell breathing. Control Syst IEEE 2004;24(2):30–46. http://dx.doi.org/10.1109/MCS.2004.1275430.
[57] Fletcher T, Thring RH, Watkinson M, Staffell I. Comparison of fuel consumption and fuel cell degradation using an

optimised controller. ECS Trans 2016;71(1):85–97. http://dx.doi.org/10.1149/07101.0085ecst. arXiv:http://ecst.ecsdl.org/content/71/1/85.full.pdf+html.

[58] Hu X, Johannesson L, Murgovski N, Egardt B. Longevity-conscious dimensioning and power management of the hybrid energy storage system in a fuel cell hybrid electric bus. Appl Energy 2015;137:913–24. http://dx.doi.org/10.1016/j.apenergy.2014.05.013.

[59] Li Q, Yang H, Han Y, Li M, Chen W. A state machine strategy based on droop control for an energy management system of PEMFC-battery-supercapacitor hybrid tramway. Int J Hydrogen Energy 2016;41(36):16148–59. http://dx.doi.org/10.1016/j.ijhydene.2016.04.254.

[60] Wu J, Yuan X-Z, Martin JJ, Wang H, Yang D, Qiao J, et al. Proton exchange membrane fuel cell degradation under close to open-circuit conditions: part i: in situ diagnosis. J Power Sources 2010;195(4):1171–6. http://dx.doi.org/10.1016/j.jpowsour.2009.08.095.

[61] Bae SJ, Kim S-J, Park JI, Park CW, Lee J-H, Song I, et al. Lifetime prediction of a polymer electrolyte membrane fuel cell via an accelerated startup-shutdown cycle test. Int J Hydrogen Energy 2012;37(12):9775–81. http://dx.doi.org/10.1016/j.ijhydene.2012.03.104.

[62] Avakov V, Bogdanovskaya V, Kapustin A, Korchagin O, Kuzov A, Landgraf I, et al. Lifetime prediction for the hydrogen-air fuel cells. Russ J Electrochem 2015;51(6):570–86. http://dx.doi.org/10.1134/S1023193515060026.

[63] Schmittinger W, Vahidi A. A review of the main parameters influencing long-term performance and durability of PEM fuel cells. J Power Sources 2008;180(1):1–14. http://dx.doi.org/10.1016/j.jpowsour.2008.01.070.

[64] Shao Y, Yin G, Gao Y. Understanding and approaches for the durability issues of Pt-based catalysts for PEM fuel cell. J Power Sources 2007;171(2):558–66. http://dx.doi.org/10.1016/j.jpowsour.2007.07.004.

[65] Kendall K, Pollet B, Jostins J. Hydrogen hybrid vehicles for University of Birmingham campus. In: IET HEVC 2008: Hybrid and Eco-Friendly Vehicle Conference; 2008. p. 1–3.

[66] Kendall K, Pollet B, Dhir A, Staffell I, Millington B, Jostins J. Hydrogen fuel cell hybrid vehicles (HFCHV) for Birmingham campus. J Power Sources 2011;196(1):325–30. http://dx.doi.org/10.1016/j.jpowsour.2009.12.012.

[67] Staffell I. Results from the Microcab fuel cell vehicle demonstration at the University of Birmingham. Int J Electr Hybrid Veh 2011;3(1):62–82. http://dx.doi.org/10.1504/IJEHV.2011.040473.